Continuum theory of 4*mm*-2*mm* proper ferroelastic transformation under inhomogeneous stress

Wenwu Cao* and James A. Krumhansl
Laboratory of Atomic and Solid State Physics, Cornell University, Ithaca, New York 14853
(Received 5 March 1990)

We have studied a model square-rectangular proper ferroelastic transition in an inhomogeneous stress field $\sigma(\mathbf{R})$ with nonzero deviatoric stress component. This stress field can induce spatially heterogeneous transformations. Quasi-one-dimensional solutions for the lattice displacement fields $\mathbf{u}$ are derived both analytically and numerically for some special choices of stress functions. We find that the local instability is influenced by three factors: temperature, the magnitude of the applied stress, and the stress size. A critical strength $\sigma_c (=0.801$ in dimensionless units) exists such that for $|\sigma(\mathbf{R})_{\max} > \sigma_c$ a local transition can occur without an activation energy. The constraints of boundary conditions on the allowed solutions are also examined, and single-phase or twinned embryos may be formed through local transitions for free boundary conditions or fixed ends, respectively.

I. INTRODUCTION

The theory of heterogeneous displacive phase transitions in a solid system has been and continues to be a challenging problem. It is still far from being thoroughly understood despite the large amount of work done in this field. There are discrepancies and inconsistencies between theories and experiments as well as within the experiments. The complications are due to several causes: First, there are significant effects of defects in almost all systems. Second, usually a displacive phase transition in a solid, proper or improper ferroelastic, is accompanied by structural distortions, and these distortions often interact with other defect induced distortions through long-range elastic coupling, which complicates the problem in comparison with systems having only short-range interactions. Third, in many experiments, sample holder and other mechanical constraints directly influence some physical properties and, in some cases, even the nature of the phase transition; thus one must study the effect of stress, especially of heterogeneous stress.

The effects of homogeneous external stress on phase transitions has been studied by several investigations,[1-3] who have shown how the first-order transition temperature could be altered by the stress field in a proper ferroelastic system (things are different for a second-order phase transition,[4] for which the phase transition is smeared out by the applied stress).[5] As for the case of heterogeneous stress, little work has been done up to now, but it is, in reality, more relevant to the defect-induced transformation problem.[6] In a previous paper we have introduced a method to treat systems with defects and proposed a continuum model which might be used to explain the heterogeneous transformation and thermal growth process in an athermal martensite.[7] Based on that model we will, in this paper, address how boundary conditions determine the allowed solutions, and look at the effects of magnitude and extent of an applied stress on the local thermadynamic instability.

For illustrative purposes here we treat only an applied stress field with certain symmetry, i.e., the deviatoric stress in the square-rectangular phase transition. The interphase and interface boundaries are assumed to be coherent, and we neglect additional stress fields possibly generated by the transformation process. Analytic functional forms for the stress field were assumed, which might be realized either by introducing suitable substitutional or interstitial defects, or by applying surface constraints to the system. Even with such a simplified model, many observations could be correlated and better understood, including the concepts of local instability, preexisting embryos, pinning of twin boundaries by defects as well as the heterogeneity of transformations in many systems.[8,9]

The paper proceeds as follows: Section II defines the theoretical model and the equilibrium conditions. Solutions for free boundary conditions which would lead to a single domain product phase, and solutions for fixed ends which lead to a twinned product phase, are given in Sec. III and IV, respectively. The final section is the summary and conclusion.

II. 2D MODEL FOR A PROPER FERROELASTIC TRANSITION

For a proper ferroelastic transition the system free energy depend only on the elastic strain tensor

$$\eta_{i,j} = \tfrac{1}{2}(u_{i,j} + u_{j,i} + u_{k,i}u_{k,j}), \quad (i,j,k = 1,2) . \tag{1}$$

Here u_i are the components of displacement field, the indices after comma represents a partial derivative with respect to the corresponding space variable, and the last term in the parentheses is the geometrical nonlinearity. The total free energy of the system can be written, in the continuum approximation, as

$$G = \int\int g(u_{i,j}, u_{i,jk}, \sigma_{ij}) dV , \tag{2}$$

with

$$g(u_{i,j}, u_{i,jk}, \sigma_{ij}) = g_0(u_{i,j}, \sigma_{ij}) + g_G(u_{i,jk}) . \tag{3}$$

$g_0(u_{i,j}, \sigma_{ij})$ is the contribution of local strain and external

local stress, which includes both harmonic and anharmonic terms; $g_G(u_{i,jk})$ is the strain gradient energy discussed below. For the 4mm-2mm proper ferroelastic transition it is convenient to use the so-called symmetry coordinates,[10,11] in which the three independent elastic strain components are

$$e_1=\frac{1}{\sqrt{2}}(\eta_{11}+\eta_{22}) , \tag{4a}$$

$$e_2=\frac{1}{\sqrt{2}}(\eta_{11}-\eta_{22}) , \tag{4b}$$

$$e_3=\eta_{12} . \tag{4c}$$

In terms of these symmetry coordinates $g_0(u_{i,j},\sigma_{ij})$ can be written explicitly as

$$g_0(u_{i,j},\sigma_{ij})=\left[\frac{A_\alpha}{2}e_\alpha^2-\sigma_\alpha e_\alpha\right]+\frac{B}{4}e_2^4+\frac{C}{6}e_2^6 \quad (\alpha=1,2,3) , \tag{5}$$

where summation convention has been used, and the coefficients

$$A_1=c_{11}+c_{12}, \quad A_2=c_{11}-c_{12}, \quad A_3=c_{33} \tag{6}$$

are the independent combinations of second order elastic constants for square symmetry in Voigt notation, σ_α ($\alpha=1,2,3$) are the components of external local stress in the symmetry coordinates. The last two terms in Eq. (5) with $B<0$ and $C>0$ are the minimum anharmonic terms required in order to describe a first-order phase transition. Only those high-order terms which contain the deviatoric strain e_2 were retained in the free energy expansion for simplicity. B and C are linear combinations of fourth and sixth-order elastic constants.

For the same reason only the lowest-order strain gradient terms are kept in the energy expansion, so that the gradient energy $g_G(u_{i,jk})$ is given by[11]

$$\begin{aligned} g_G(e_{\alpha,i})=&\tfrac{1}{2}d_1(e_{1,1}^2+e_{1,2}^2)+\tfrac{1}{2}d_2(e_{2,1}^2+e_{2,2}^2) \\ &+\tfrac{1}{2}d_3(e_{3,1}^2+e_{3,2}^2)+d_4(e_{1,1}e_{2,1}-e_{2,1}e_{2,2}) \\ &+d_5(e_{1,1}e_{3,2}+e_{1,2}e_{3,1}) \\ &+d_6(e_{2,1}e_{3,2}-e_{3,2}e_{3,1}) \quad (\alpha=1,2,3;i=1,2) , \end{aligned} \tag{7}$$

Only four of the six strain gradient coefficients are independent and they can be determined from phonon dispersion curves by inelastic neutron scattering.[11]

One can now write down the system Lagrangian

$$L=\int[\tfrac{1}{2}\rho_0\dot{u}_i\dot{u}_i-g(u_{i,j},u_{i,jk},\sigma_{ij})]dV \quad (i,j,k=1,2) ; \tag{8}$$

again, summation conversion has been used, ρ_0 is the mass density. The equation of motion is[10,11]

$$\rho_0\ddot{u}_i=\frac{\partial}{\partial X_j}\left[\frac{\partial g}{\partial u_{i,j}}-\frac{\partial}{\partial X_k}\frac{\partial g}{\partial u_{i,jk}}\right] \quad (i,j,k=1,2) . \tag{9}$$

For static configurations we set the left side of Eq. (9) to be zero.

In a 4mm-2mm proper ferroelastic martensitic transformation, the lattice motion is a pure $\langle 11\rangle/\langle 1\bar{1}\rangle$ shear, and there are two low-temperature variants which are energetically degenerate in the absence of external stress or body force. Consider now an infinite long slab with the dimension $L_l\to\infty$ and $L_s\ll L_l$, to be in the directions of $\langle 11\rangle$ and $\langle 1\bar{1}\rangle$, respectively, and apply an external stress σ_2 to lift the twofold degeneracy. A quasi-one-dimensional solution can be found under the approximation of geometrical linearity [i.e., neglecting the product term in Eq. (1)], for example,[7] if

$$\sigma_2=\sigma_2(\hat{\mathbf{n}}\cdot\mathbf{R})>0, \text{ with } \hat{\mathbf{n}}=\frac{1}{\sqrt{2}}(1,1) , \tag{10}$$

the displacement field $\mathbf{u}$ may be given by

$$\mathbf{u}=\hat{\mathbf{m}}v(\hat{\mathbf{n}}\cdot\mathbf{R}), \text{ with } \hat{\mathbf{m}}=\frac{1}{\sqrt{2}}(1,\bar{1}) . \tag{11}$$

Defining a new variable $X'=\hat{\mathbf{n}}\cdot\mathbf{R}$, one can derive the strain components e_α according to Eqs. (4a–c) and (11) to be

$$e_1=0, \quad e_2=\frac{1}{\sqrt{2}}\frac{d}{dX'}v(X'), \quad e_3=0 . \tag{12}$$

This is to say that the phase transition is area conserving and has no shear strain.

Substituting Eq. (12) into Eq. (5) leads to an effective elastic ϕ^6 model under stress with single component order parameter e_2. In the absence of stress ($\sigma_2=0$) for that model the first-order phase transition temperature T_1 is given by[12]

$$T_1=T_c+\frac{3B^2}{16\beta C} , \tag{13}$$

where β is positive and independent of temperature, and is related to A_2 through the relation $A_2=\beta(T-T_c)$.

When $\sigma_2(X')\neq 0$ but is localized (nonzero only within certain range), we would still expect the bulk transition temperature to be the same as Eq. (13) except inside the range of the stress field. Outside that region for $T>T_1$ the system is in the high-temperature square phase at $X'=\pm\infty$, which defines the boundary condition for solutions above T_1,

$$\lim_{X'\to\pm\infty} e_2=0 . \tag{14}$$

By substituting the results of Eq. (12) into Eq. (9) and integrating it once using the boundary condition Eq. (14), one can simplify the equilibrium condition to give a second-order ordinary differential equation

$$d_2\frac{d^2e_2}{dX'^2}=A_2e_2+Be_2^3+Ce_2^5-\sigma_2(X') . \tag{15}$$

We shall discuss different solutions of Eq. (15) in the two following sections in conjunction with the relevant boundary conditions.

III. SOLUTION FOR FREE BOUNDARY CONDITIONS ABOVE T_1

The simplest case would be the insertion of a single line of foreign atoms at $X'=0$. If the produced stress field can be approximated as

$$\sigma_2(X')=\sigma_0\delta(X') , \tag{16}$$

one can solve Eq. (15) analytically to give

$$e_2=\left[\frac{2A_2(B+2W)}{W^2-\frac{4}{3}A_2C}\right]^{1/2} , \tag{17}$$

with

$$W=W_0e^{2\sqrt{A_2/d_2}|X'|}-\frac{B}{2} . \tag{18}$$

Clearly $e_2\to 0$ as $|X'|\to\infty$. The constant W_0 can be determined by putting Eq. (18) back to Eq. (15), and integrating Eq. (15) once over the range $-\Delta<X'<\Delta$ then taking the limit $\Delta\to 0$, which gives the condition

$$\frac{8A_2\sqrt{W_0d_2}(W_0^2-B^2/4+\frac{4}{3}A_2C)}{[(W_0-B/2)^2-\frac{4}{3}A_2C]^{3/2}}=\sigma_0 . \tag{19}$$

Using Eqs. (11), (12), and (17) one can easily derive the displacement field $\mathbf{u}$,

$$\mathbf{u}=\hat{\mathbf{m}}v(X') ; \tag{20}$$

$$v(X')=\begin{cases}\sqrt{d_2/a}\,F(\nu,q), & \text{for } X'\le 0,\\ \sqrt{d_2/a}\,[2F(\nu_0,q)-F(\nu,q)], & \text{for } X'>0,\end{cases}$$

where $F(\nu,q)$ is the elliptic integral of the first kind and

$$a=\sqrt{\tfrac{4}{3}A_2C} , \tag{21a}$$

$$b=-\frac{B}{2} , \tag{21b}$$

$$q=\left[\frac{b+a}{2a}\right]^{1/2} , \tag{21c}$$

$$\nu_0=\arcsin\left[\frac{2a}{W_0+a}\right]^{1/2} , \tag{21d}$$

$$\nu=\arcsin\left[\frac{2a}{W+a}\right]^{1/2} . \tag{21e}$$

Equation (20) is a kink which describes the local destortion of the high-temperature phase with a δ-function stress acts at $X'=0$. This distortion will cause a relative shift of the system at $X'\neq 0$ [similar to the picture given in Fig. (5a)]. However, the size of the distortion does not change significantly with temperature, and the magnitude W_0 is a continuous function of temperature through A_2 [Eq. (19)], therefore, this local distortion does not induce a local transition and can not be considered as the embryo of the low-temperature phase. The reason, as will be shown later, is because the assumed stress field Eq. (16) has no width. In reality a δ function is not a good description of the physical picture, the stress should have both finite magnitude and width, so that the discontinuity of strain gradient resulting from δ-function stress will be smoothed out, and a local transition can be induced.

Unfortunately, analytic solutions can not be found for a general functional form of $\sigma_2(X')$, so numerical methods have been used. As an example, we took a model function

$$\sigma_2(X')=\sigma_0\operatorname{sech}\frac{X'}{X_0'} , \tag{22}$$

where σ_0 and X_0' describe the strength and characteristic width of the stress field, respectively. For convenience the physical quantities are then rescaled to dimensionless form according to the following transformations:

$$\epsilon=\left[\frac{4C}{-3B}\right]^{1/2}e_2 , \tag{23a}$$

$$\tau=\frac{T-T_c}{T_1-T_c} , \tag{23b}$$

$$\hat{\sigma}_0=\frac{16C}{3B^2}\left[\frac{4C}{-3B}\right]^{1/2}\sigma_0 , \tag{23c}$$

$$\xi=X'/\gamma,\quad \gamma^2=\frac{16Cd_2}{3B^2} . \tag{23d}$$

It is found that there are three factors which influence the heterogeneous phase transition process, the system temperature τ (homogeneous), the strength of the stress field $\hat{\sigma}_0$ and the characteristic range of the stress ξ_0. We will address them individually.

A. Temperature-induced heterogeneous phase transition

First, let us fix the strength and width of the stress, then examine how the transition proceeds with decreasing temperature. The results for a choice of $\hat{\sigma}_0=0.6$ and $\xi_0=2$ are shown in Fig. 1 in a half space (the solution are all even function of ξ). For $\tau>\tau_s=1.7558$, the local distortions caused by the stress field increase on cooling, but very slow. At $\tau=\tau_s$ a first-order transition occurs, which transforms the local distortion into an embryo of the low-temperature phase. Further cooling ($1<\tau<\tau_s$) produces the thermal growth of this embryo,[7] and at $\tau=\tau_1=1$ (the rescaled bulk transition temperature without external stress) the whole system transforms into a single-domain low-temperature phase. Note here the interface of low- and high-temperature phases is assumed to be coherent.

B. Stress-induced heterogeneous transition

Next, we look at the case for which the width of stress and the temperature of the system are fixed but vary the magnitude of the stress field $\hat{\sigma}_0$. In certain temperature range above τ_1, stress induced local transition is possible. Figure 2 illustrates the transition process, for which the temperature and range of stress are chosen to be $\tau=1.5$ and $\xi_0=2$. It can be seen clearly that the maximum strain value $\epsilon(0)$ at $\xi=0$ experiencing a discontinuous

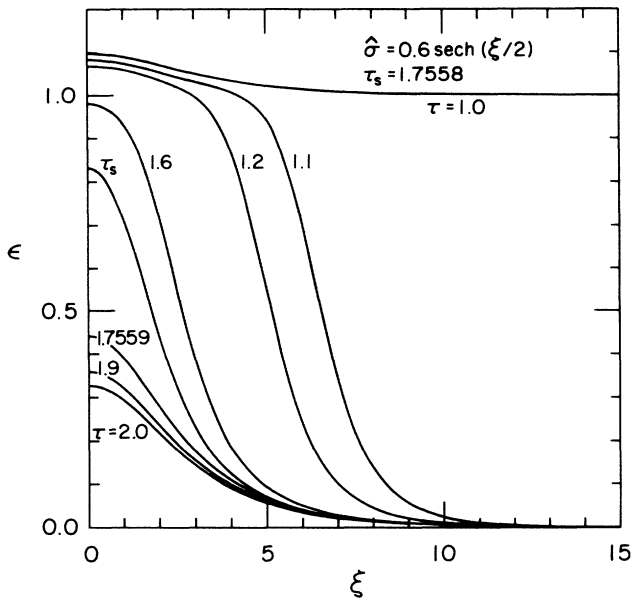

FIG. 1. Profiles of rescaled deviatoric strain ϵ vs distance ξ from the defect center for different temperatures τ. The local distortion transforms into embryo of the low-temperature phase at $\tau_s = 1.7588$ for parameters $\hat{\sigma}_0 = 0.6$ and $\xi_0 = 2$. Plots for negative ξ can be obtained by the relation $\epsilon(-\xi) = \epsilon(\xi)$.

jump when the stress magnitude increases to $\hat{\sigma}_0 = 0.4068$, which implies a stress induced local first-order transition. Further increase of $\hat{\sigma}_0$ produces greater (localized) deformation of the low-temperature embryo, but the size of the embryo is not influenced much. To a certain extent the effect of increasing $\hat{\sigma}_0$ is equivalent to decreasing τ in a limited range of $\hat{\sigma}_0$ and τ. But one must remember that the applied stress should be within the elastic limit of the system, i.e., no plastic deformation is allowed in the present model.

C. Local transition temperature τ_s and critical stress $\hat{\sigma}_c$

The strain space profile $\epsilon(\xi)$, which minimizes the total energy, is a hump resulting from the stress Eq. (22). When $\hat{\sigma}_0$ is small, an energy barrier exists in order parameter space, which makes certain strain space profiles thermadynamically unstable. If we use the height of the hump $\epsilon(0)$ to characterize these profiles, a discontinuity will occur at $\tau = \tau_s$, thus we define τ_s to be the local transition temperature. Figure 3 shows the plots of $\epsilon(0)$ versus τ for several $\hat{\sigma}_0$ with $\xi_0 = 2$. One can see that τ_s increases with $\hat{\sigma}_0$, and at the same time the discontinuity of $\epsilon(0)$ becomes smaller. There is a critical strength $\hat{\sigma}_c$, for $\hat{\sigma}_0 > \hat{\sigma}_c$ the discontinuity disappears and the transition becomes continuous. This corresponds to the physical situation for which the free energy density at $\xi = 0$ has only one minimum with respect to the local order parameter at any temperature. We found this critical stress to be $\hat{\sigma}_c = 0.801$ in dimensionless units, which naturally is consistent with the case of a system under homogeneous stress.[7] The continuous growth of the strain profile with lowering temperature signifies the loss of transformation barrier. Therefore, we define those local distortions caused by stress magnitude $\hat{\sigma}_0 > 0.801$ to be the embryos of the low-temperature phase, because a transition temperature τ_s can no more be defined.

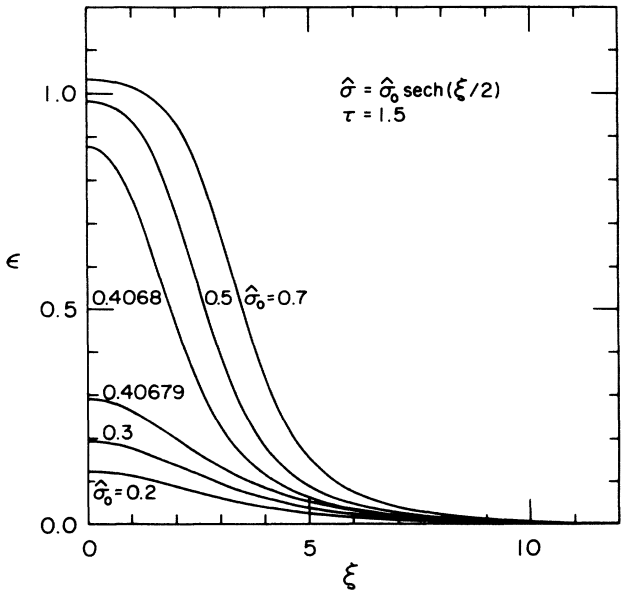

FIG. 2. Stress-induced local transformation at temperature $\tau = 1.5$. The critical stress magnitude is $\hat{\sigma}_0 = 0.4068$ in dimensionless units.

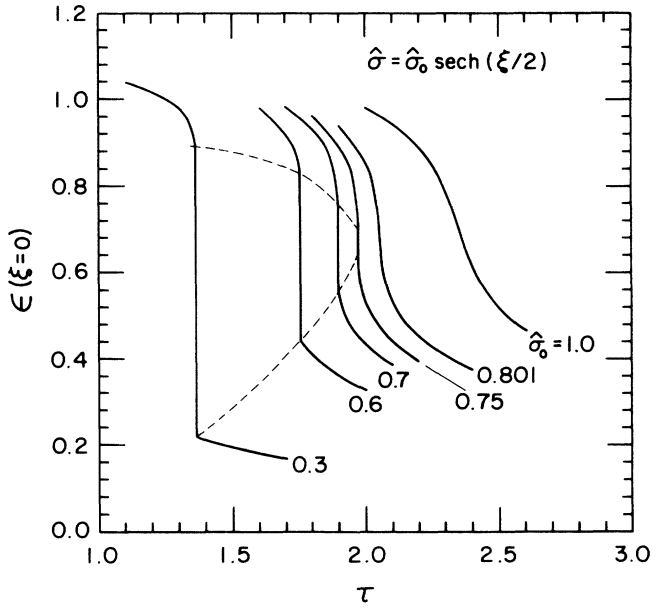

FIG. 3. The magnitude of stress profile, $\epsilon(\xi = 0)$ vs temperature τ for different stress magnitude $\hat{\sigma}_0$. The discontinuity of $\epsilon(0)$ is the signature of the local first-order transition, which becomes smaller as $\hat{\sigma}_0$ increases. The critical stress magnitude is defined to be $\hat{\sigma}_c = 0.801$ in dimensionless unit. For $\hat{\sigma}_0 > \hat{\sigma}_c$, $\epsilon(0)$ becomes a continuous function of τ.

D. Effect of stress range ξ_0 on the phase transition

The range of the applied stress is also very important; it affects the total system gradient energy associated with the local distortion. When $\hat{\sigma}_0 > 0.801$, the energy density has only one minimum with respect to the local order parameter, so that the space profile of the strain order parameter will continuously grow following the shift of this minimum with decreasing temperature. However, the growth rate is greatly influenced by the size of the stress field. Only $\hat{\sigma}_0 < 0.801$, can a local transition temperature τ_s be defined. One can clearly see the strong size effect shown in Fig. 4. Generally speaking, the local transformation can be induced by stress either larger in magnitude ($\hat{\sigma}_0$) but smaller in extent (ξ_0), or smaller in magnitude but larger in extent, which is partly in analogy with the fluctuation mediated classical nucleation theory.[13] However, there are two points need to be addressed: One is that for very small size stress ($\xi_0 < 0.1$), the local transition temperature is not too much different from that of the bulk, so the stressed regions would only provide nucleation centers for the bulk transformation and prevent the system from supercooling. The other is that for stress of larger ξ_0 (> 10), the size effect diminishes and the magnitude $\hat{\sigma}_0$ becomes the dominant factor to control the local transition. As $\xi_0 \to \infty$ the system becomes homogeneous with a constant stress $\hat{\sigma}_0$, and so the transition temperature for a given $\hat{\sigma}_0$ reaches the asymptotic value given in Fig. 2 of our previous paper.[7]

E. The displacement field

The displacement field **u** corresponding to the results of Figs. 1 and 2 can be easily calculated from Eqs. (11) and (12). A typical result is shown in Fig. (5a) for an intermediate temperature between τ_s and τ_f, i.e., $\tau_s > \tau > \tau_f$, where τ_f is the bulk transformation temperature and $\tau_f = \tau_1 = 1$ for an infinite system ($L_l \to \infty$) but $\tau_f > 1$ for a finite system. It is important to see the relative shift of the two ends caused by the partial square-rectangular transition in Fig. 5(a). As the transformation proceeds in space, this shift becomes larger, and it diverges for an infinite system. Therefore, solutions given in Fig. 1 as well as Eq. (20) can only exist with free ends, for which the transverse translation of the system does not cost energy. When the relative position of the two ends are fixed, these solutions are not allowed, so we must consider that case anew.

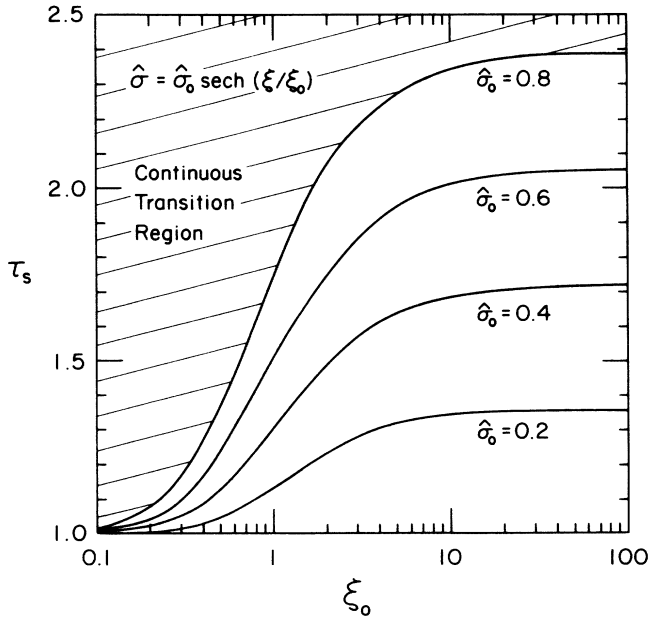

FIG. 4. Local transition temperature τ_s vs the characteristic width ξ_0 of the stress field for different $\hat{\sigma}_0$. τ_s increases with $\hat{\sigma}_0$ but becomes undefined for $\hat{\sigma}_0 > \hat{\sigma}_c$ (shaded area).

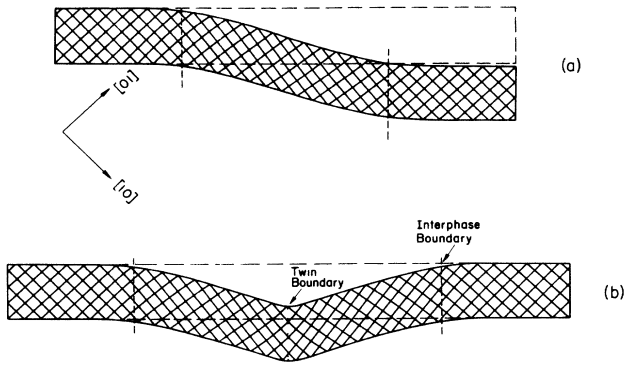

FIG. 5. Illustration of lattice displacements pattern represented by (a) Solutions in Fig. 1; (b) Solutions in Fig. 6.

IV. SOLUTIONS FOR FIXED ENDS ABOVE T_1

When the two ends of the rectangular slab are fixed at $X' = \pm\infty$, the displacement field **u** must be an even function with respect to space variable, so that the corresponding strain becomes an odd function. Physically, this means that $X' > 0$ corresponds to one variant, $X' < 0$ to the another. One can see from Eq. (15) that the space parity of e_2 is determined by the parity of $\sigma_2(X')$. Therefore, in order to form a twin seed, $\sigma_2(X')$ must be an odd function. We choose, for convenience, the derivative form of Eq. (22) as a model function (in fact any odd function will do)

$$\sigma_2(X') = \sigma_0 \operatorname{sech}\left[\frac{X'}{X'_0}\right] \tanh\left[\frac{X'}{X'_0}\right] \tag{24}$$

to show the characteristics of a twin solution and its thermal growth process. The numerical results are given in Fig. 6 with the parameters chosen as $\hat{\sigma}_0 = 0.6$, and $\xi_0 = 4$. Here we have doubled the range of the stress function because the size effect strongly suppresses τ_s. With the above parameters we found the temperature of forming the twin embryo of low-temperature phase is $\tau_s = 1.3782$. Again coherency in both the twin boundary and the two interphase boundaries has been assumed. It is interesting to point out the different behavior of the twin boundary and of the interphase boundaries. The twin boundary is fixed in space, or "pinned" by the ap-

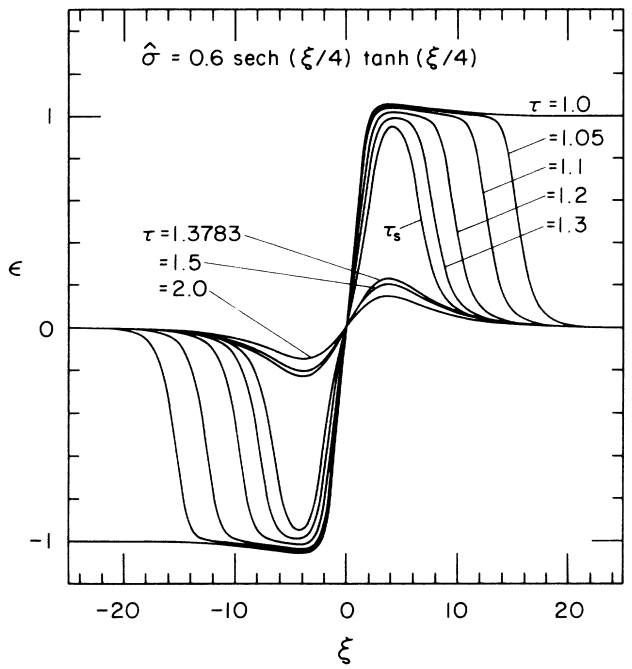

FIG. 6. The strain profiles $\epsilon(\xi)$ for a twinned embryo at different temperatures under the stress field given by Eq. (25) for parameters $\hat{\sigma}_0=0.6$ and $\xi_0=2$. The local transition temperature is $\tau_s=1.3782$.

plied (or defect) stress, but the two interphase boundaries move away from each other with further cooling, representing the thermal growth of the equilibrium size of this twinned embryo. The final product phase is a bicrystal. When lateral constraints are present, this will not be possible because the large displacement of the lattice near the twin boundary [see Fig. (5b)]. In this case, a twin band could be formed[14,15] in order to minimize the (macroscopic) transformation strain.

The analyses for the effects of $\hat{\sigma}_0$ and ξ_0 can be carried out easily in the same way as in Sec. III. Similar results as Figs. 3 and 4 have been obtained.

V. SUMMARY AND CONCLUSIONS

Through the above analyses we conclude that a "phase diagram" which describes the heterogeneous transformation process under inhomogeneous stress must involve three parameters: the system temperature τ, the strength of the stress field $\hat{\sigma}_0$ and the characteristic range ξ_0 of the applied stress. There exists a critical strength $\hat{\sigma}_c$; for $\hat{\sigma}_0<\hat{\sigma}_c$ the local distortion transforms into an embryo of the low-temperature phase via a first-order transition, which can be triggered by thermal fluctuations; for $\hat{\sigma}_0>\hat{\sigma}_c$ this transformation is smeared out, and the local distortion simply grows continuously into a region of the low-temperature phase upon lowering temperature. Since thermal fluctuations are not necessary for the latter case, one could view the local distortions caused by large stress ($\hat{\sigma}_0>\hat{\sigma}_c$) as the preexisting embryo of the low-temperature phase.[16–18] One may notice that the symmetries of local distortion and the embryo are the same, τ_s is defined as the temperature at which the maximum value of the equilibrium strain space profile experiences a jump. As $\hat{\sigma}_0$ increases, this jump reduces, and finally the signature of the first-order phase transition disappears when the stress magnitude exceeds the critical value $\hat{\sigma}_c$. In laboratory units σ_c ($\sim$0.801 in dimensionless units) depends on system parameters according to Eq. (23c). In general, this critical stress is small, for instance, $\sigma_c\sim 5$ bar for $In_{0.79}Tl_{0.21}$. We have also calculated the conversion factor γ in Eq. (23d) for the same material, which is roughly $\gamma\sim a/2$, where a is the lattice constant. If we characterize the stress size by $2\xi_0$, one can conclude from Fig. 4 that for $In_{0.79}Tl_{0.21}$ the size effect becomes insignificant when the stress range is greater than ten lattice constants, but for smaller range stresses this size effect strongly affects the local transition temperature τ_s or the growth rate of an embryo (large $\hat{\sigma}_0$).

In the past, people have attempted to develop a scheme parallel to the theory of liquid-vapor transformations to apply to a solid system.[19–23] However, that kind of theory often has led to an unphysical energy barrier.[23,24] More importantly, the phenomena of partial transformation, viz., the equilibrium coexistence of mixed high- and low-temperature phases in a certain temperature range, as well as the phenomena of transformation precursors are beyond the capability of such classical theories. Other attempts, such as local soft mode[25] and preexisting embryo theory,[16–18] may provide a partial understanding of the problem (despite many remaining questions in those models) but remain to be correlated. Though idealized, the model we have presented here may help to provide a conceptual link between these different physical concepts, to the extent that they are defect controlled through inhomogeneous elastic stresses.

Finally, to summarize, defects create local stresses which cause the local distortions of the host matrix. These local distortions can become the sites of local instability. We have shown in the present pedagogical model that the local instability temperature τ_s is not separately defined, but depends on both the strength and the range of applied stress field. Together with the fact that defect concentrations and boundary conditions are different for each sample, it is apparent why τ_s is generally sample dependent.

A real system contains many defects which induce localized stress fields and hence local distortions. However, whether a particular distortion around defects is allowed to transform or grow into the low-temperature phase is determined also by the boundary conditions on the system. Here, we have looked at two simple cases, free boundaries and fixed ends; for each the lateral dimensions were assumed free of constraints, which is to say that the lattices can be translated in L_s dimension without causing additional elastic energy. That is generally not true, and in practice the local transformed regions are subject to constraints from all sides. This will produce a twin band product phase, no matter what the parity of the original distortion is, in order to minimize the induced global elastic energy. It is evident that defects of large

size, which are the favored local instability sites, have very low mobility. The twin pattern grown from these stress centers would have relatively stable positions in space and be reproducible upon temperature recycling. Because of the pinning (Fig. 5b) provided by these low mobility defects, a finite energy is required to move the final product twin pattern, which could influence shape memory behavior.

ACKNOWLEDGMENTS

This research was supported by the U.S. Department of Energy under Contract No. De-FG02-88-ER45364.

*Present address: Materials Research Laboratory, The Pennsylvania State University, University Park, PA 16802.

[1]J. R. Patel and M Cohen, Acta Metall. **1**, 531 (1953).
[2]N. Szabo, J. Phys. C **8**, L397 (1975).
[3]B. Pietrass, Phys. Status Solidi B **68**, 553 (1975).
[4]J. R. Patel and B. W. Batterman, J. Appl. Phys. **37**, 3447 (1966).
[5]F. Falk, J. Phys. Colloq. **43**, C4-3 (1982).
[6]A. P. Levanyuk, A. S. Sigov, and A. A. Sobyanin, Ferroelectrics **24**, 61 (1980).
[7]W. Cao, J. A. Krumhansl, and R. J. Gooding, Phys. Rev. B **41**, 11 319 (1990).
[8]T. Saburi and S. Nenno, in *Proceedings of the International Conference on Martensitic Transformations (ICOMAT-86)*, edited by I. Tamura (Japan Institute of Metals, Sendai, 1987), p. 671.
[9]L. E. Tanner (private communication).
[10]A. E. Jacobs, Phys. Rev. B **31**, 5984 (1985).
[11]G. R. Barsch and J. A. Krumhansl, Metal. Trans. **19A**, 761 (1988).
[12]F. Falk, Z. Phys. B **51**, 177 (1983).
[13]J. W. Gibbs, *The Scientific Papers of J. W. Gibbs* (Longmans Green and Co., New York, 1906), Vol. 1, p. 105.
[14]G. R. Barsch, B. Horovitz, and J. A. Krumhansl, Phys. Rev. Lett. **59**, 1251 (1987).
[15]B. Horovitz, G. R. Barsch, and J. A. Krumhansl, Phys. Rev. B **42** (to be published).
[16]L. Kaufman and M. Cohen, Prog. Metal Phys. **7**, 165 (1958).
[17]V. Raghavan and M. Cohen, Scr. Metall. **7**, 591 (1973).
[18]G. B. Olson and Morris Cohen, Metall. Trans. A **7**, 1897 (1976).
[19]R. Becker and W. Doering, Ann. Phys. (N.Y.) **24**, 719 (1935).
[20]D. Turnbull and J. C. Fisher, J. Chem. Phys. **17**, 71 (1949).
[21]D. Turnbull, Trans. Am. Phys. **22**, 1614 (1954).
[22]H. Wakeshima, J. Phys. Soc. Jpn. **9**, 200 (1954).
[23]A. Kantrowitz, J. Chem. Phys. **19**, 1097 (1951).
[24]H. Knapp and U. Dehlinger, Acta. Metall. **4**, 289 (1956).
[25]P. C. Clapp, Phys. Status Solidi B **57**, 561 (1973).
[26]J. Lajzerowicz, Ferroelectrics **35**, 219 (1981).
[27]Wenwu Cao, G. R. Barsch, and J. A. Krumhansl, Phys. Rev. B **42** (to be published).